Kinetics of 1,4-Hydrogen Migration in the Alkyl Radical Reaction Class

Barbara Bankiewicz,[†] Lam K. Huynh,[‡] Artur Ratkiewicz,[†] and Thanh N. Truong*[,‡]

Henry Eyring Center for Theoretical Chemistry, Department of Chemistry, University of Utah, 315 South 1400 East Room 2020, Salt Lake City, Utah 84112 and Chemistry Institute, University of Bialystok, Hurtowa 1 15-399 Bialystok, Poland

Received: October 7, 2008; Revised Manuscript Received: November 18, 2008

The kinetics of the 1,4-intramolecular hydrogen migration in the alkyl radicals reaction class has been studied using reaction class transition-state theory combined with the linear energy relationship (LER) and barrier height grouping (BHG) approach. The rate constants for the reference reaction of n-C_4H_9 were obtained by canonical variational transition-state theory (CVT) with the small curvature tunnelling (SCT) correction in the temperature range 300−3000 K with potential-energy surface information computed at the CCSD(T)/cc-pVDZ//BH&HLYP/cc-pVDZ level of theory. Error analyses indicate that RC-TST/LER, where only reaction energy is needed, and RC-TST/BHG, where no other information is needed, can predict rate constants for any reaction in this reaction class with excellent accuracy. Specifically, for this reaction class the RC-TST/LER method has less than 65% systematic errors in the predicted rate constants, while the RC-TST/BHG method has less than 80% error when compared to explicit rate calculations.

Introduction

Isomerization, via intramolecular hydrogen-atom migration, forms an important class of alkyl and alkenyl radical reactions. It has long been known that these reactions are of importance in various complex reaction systems such as combustion of hydrocarbons.[1−4] Formation of some products in such systems can be explained only in terms of isomerization.[5] Hydrogen shift reactions were also found to play a significant role in determining the product distribution in the last stage of paraffin pyrolyses. Furthermore, radical isomerization appears to compete in hydrocarbon oxidation systems with radical decomposition and can be quite often encountered in the postulation of the mechanism of the processes involving radical intermediates.[6] Determination of the thermal rate coefficients of these isomerization reactions is a prerequisite for modeling of systems such as engines and furnaces operating with hydrocarbon fuels.

In spite of the latest experimental achievements relatively little information is currently available for the kinetics of intramolecular hydrogen-transfer reactions despite their importance. This is because direct measurements of the rate constants of isomerization are difficult due to competing reactions. Most of the rate parameters for isomerization processes in the literature were derived from analysis of the chain reaction systems and sometimes suffered from the inadequacy of the kinetic models used.[7−13] For that reason, the accuracy of older data is questionable.[7−14] Significant progress in experimental work has been done by Tsang and co-workers on pentyl-,[15] hexyl-,[16] heptyl-,[17] octyl-,[14] and 4-methyl-1-pentyl radicals.[18] High-pressure limit rate constants for 1,4-H shift were proposed by Tsang and co-workers with a quoted uncertainty of less than a factor of 2.

There are a number of theoretical studies on the activation energies and geometries of the transition states of H-shift reactions in alkyl radicals. Viskolcz et al.[19,20] calculated the ab initio activation barriers and ring strain energies of the 1,2-, 1,3-, 1,4-, and 1,5-H-atom-transfer reactions of ethyl-, propyl-, butyl-, pentyl-, and 2-methylhexyl radicals, respectively. Pressure-dependent thermal rates were calculated for 2-methylhexyl radical.

The authors showed that the barrier height decreases as the number of atoms in the ring of the cyclic transition structure increases. A similar conclusion was derived by Curran et al.[3,4] in their series of proposed hydrocarbon combustion mechanisms. Curran et al.[3,4] approximated the activation energies for isomerization reactions in terms of the number of atoms in the transition-state ring structure (including the H atom) and type of site at which the transferred H atom was initially located. Green et al.[21] developed a set of generic rules to estimate high-pressure kinetic parameters of intermolecular hydrogen shifts (from 1,2 to 1,6) in alkyl radicals. These rules were derived from the results of DFT quantum chemistry calculations. TST calculation was performed for the 1,4-shift reaction in butyl radical C_4H_9. Subsequent rate rules in the family used the same A and n parameters in the $AT^n \exp(-E_a/RT)$ rate expression. Such a practice assumed that the neutral H shift for a primary carbon is sufficient to capture the dominant entropic effects of this type of reactions.

The aim of this study is to apply reaction class transition-state theory (RC-TST) to derive parameters for estimating the rate constants of any arbitrary reaction belonging to the 1,4-intramolecular hydrogen migration in the alkyl radicals reaction class. This is done by first deriving analytical correlation expressions for rate constants of the reference reaction with those in a small representative set of the class from explicit direct ab initio dynamics calculations of rate constants for all reactions in this representative set. The assumption is that these correlation expressions are applicable to all reactions in the class. To date, this assumption has shown to be valid.[22−27] To develop RC-TST/LER parameters for the 1,4 H-shift reaction class, 19 reactions were selected to form the representative set, Table 1.

The reference reaction is the H shift in n-C_4H_9 radical (R1). Of these 19 reactions, 8 represent H migration from a primary

* To whom correspondence should be addressed. E-mail: Thanh.Truong@utah.edu.
[†] University of Bialystok.University of Utah.
[‡] University of Utah.

10.1021/jp808874j CCC: $40.75
Published on Web 02/04/2009

TABLE 1

R_1	$CH_3CH_2CH_2CH_2^{\bullet} \rightarrow CH_2^{\bullet}CH_2CH_2CH_3$
R_2	$CH_3CH_2CH_2CH_2CH_2^{\bullet} \rightarrow CH_3CH^{\bullet}CH_2CH_2CH_3$
R_3	$CH_3CH^{\bullet}CH_2CH_2CH_3 \rightarrow CH_3CH_2CH_2CH_2CH_2^{\bullet}$
R_4	$CH_3CH_2CH^{\bullet}CH_2CH_2CH_3 \rightarrow CH_3CH_2CH_2CH_2CH_2CH_2^{\bullet}$
R_5	$(CH_3)_2CHCH_2CH^{\bullet}CH_3 \rightarrow CH_2^{\bullet}CH(CH_3)CH_2CH_2CH_3$
R_6	$CH_2^{\bullet}CH(CH_3)CH_2CH_2CH_3 \rightarrow (CH_3)_2CHCH_2CH^{\bullet}CH_3$
R_7	$(CH_3)_2CH_2CH_2CH_2CH_2^{\bullet} \rightarrow (CH_3)_2CH^{\bullet}CH_2CH_2CH_3$
R_8	$(CH_3)_2CH^{\bullet}CH_2CH_2CH_3 \rightarrow (CH_3)_2CH_2CH_2CH_2CH_2^{\bullet}$
R_9	$CH_3CH_2CH(CH_3)CH_2CH_2^{\bullet} \rightarrow CH_3CH^{\bullet}CH(CH_3)CH_2CH_3$
R_{10}	$CH_3CH^{\bullet}CH(CH_3)CH_2CH_3 \rightarrow CH_3CH_2CH(CH_3)CH_2CH_2^{\bullet}$
R_{11}	$(CH_3)_2CHCH_2CH_2CH_2^{\bullet}CH_3 \rightarrow (CH_3)_2C^{\bullet}CH_2CH_2CH_2CH_3$
R_{12}	$(C_2H_5)(CH_3)CHCH_2CH_2CH_2^{\bullet} \rightarrow (C_2H_5)\ (CH_3)C^{\bullet}CH_2CH_2CH_3$
R_{13}	$CH_3CH_2CH_2CH^{\bullet}CH_2CH_2CH_2CH_3 \rightarrow CH_2^{\bullet}CH_2CH_2CH_2CH_2CH_2CH_2CH_3$
R_{14}	$CH_2^{\bullet}CH_2CH_2CH_2CH_2CH_2CH_2CH_3 \rightarrow CH_3CH_2CH_2CH^{\bullet}CH_2CH_2CH_2CH_3$
R_{15}	$CH_3CH_2CH_2CH_2CH_2CH_2CH_2CH_2CH_2^{\bullet} \rightarrow CH_3CH_2CH_2CH_2CH_2CH^{\bullet}CH_2CH_2CH_3$
R_{16}	$CH_3CH_2CH_2CH_2CH_2CH^{\bullet}CH_2CH_2CH_3 \rightarrow CH_3CH_2CH_2CH_2CH_2CH_2CH_2CH_2^{\bullet}$
R_{17}	$(CH_3)_2CHCH_2CH_2CH_2CH_2CH_2CH_2^{\bullet} \rightarrow (CH_3)_2CHCH_2CH_2CH^{\bullet}CH_2CH_2CH_3$
R_{18}	$(CH_3)_2CH_2CH_2CH_2CH_2CH^{\bullet}CH_2CH_2CH_3 \rightarrow (CH_3)_2CH_2CH_2CH_2CH_2CH_2CH_2CH_2^{\bullet}$
R_{19}	$(CH_3CH_2CH_2CH_2)(CH_3)CHCH_2CH_2CH_2^{\bullet} \rightarrow (CH_3CH_2CH_2CH_2)(CH_3)C^{\bullet}CH_2CH_2CH_3$

C atom (type p), 7 from a secondary carbon (type s), and 4 from a tertiary carbon (type t).

Methodology

Reaction Class Transition-State Theory. Since the details of the RC-TST method have been presented elsewhere,[22,28] we discuss only its main features here. It is based on the realization that the reaction in the same class has the same reactive moiety; thus, the difference between the rate constants of any two reactions is mainly due to differences in the interactions between the reactive moiety and their different substituents. Within the RC-TST framework the rate constant of an arbitrary reaction (denoted as k_a) is proportional to the rate constant of a reference reaction, k_r, by a temperature-dependent function $f(T)$

$$k_a(T) = f(T)k_r(T) \tag{1}$$

One often would choose the reference reaction to be the smallest reaction in the class since their rate constants can be calculated accurately from first principles. The key idea of the RC-TST method is to factor $f(T)$ into different components under the TST framework

$$f(T) = f_\sigma f_\kappa f_Q f_V \tag{2}$$

where f_σ, f_κ, f_Q, and f_V are the symmetry number, tunneling, partition function, and potential-energy factors, respectively. These factors are simply the ratios of the corresponding components in the TST expression for the two reactions

$$f_\sigma = \frac{\sigma_a}{\sigma_r} \tag{3}$$

$$f_\kappa(T) = \frac{\kappa_a(T)}{\kappa_r(T)} \tag{4}$$

$$f_Q(T) = \frac{\left(\frac{Q_a^{\ddagger}(T)}{\Phi_a^{R}(T)}\right)}{\left(\frac{Q_r^{\ddagger}(T)}{\Phi_r^{R}(T)}\right)} = \frac{\left(\frac{Q_a^{\ddagger}(T)}{Q_r^{\ddagger}(T)}\right)}{\left(\frac{\Phi_a^{R}(T)}{\Phi_r^{R}(T)}\right)} \tag{5}$$

$$f_V(T) = \exp\left[-\frac{(\Delta V_a^{\ddagger} - \Delta V_r^{\ddagger})}{k_B T}\right] = \exp\left[-\frac{\Delta\Delta V^{\ddagger}}{k_B T}\right] \tag{6}$$

where $\kappa(T)$ is the transmission coefficient accounting for the quantum mechanical tunnelling effects, σ is the reaction symmetry number, $Q^{\ddagger}$ and Φ^R are the total partition functions (per unit volume) of the transition state and reactants, respectively, $\Delta V^{\ddagger}$ is the classical reaction barrier height, T is the temperature in Kelvin, and k_B and h are the Boltzmann and Planck constants, respectively. The potential-energy factor can be calculated using the reaction barrier heights of the arbitrary reaction and the reference reaction. The classical reaction barrier height $\Delta V^{\ddagger}$ for the arbitrary reaction can be obtained using the linear energy relationship (LER) similar to the well-known Evans−Polanyi linear free-energy relationship[15−17] between classical barrier heights and reaction energies of reactions. Using LER the classical barrier height for any reaction can be estimated using only the reaction energy information.

Computational Details. All electronic structure calculations were carried out using the GAUSSIAN 03 suite of programs.[29] Hybrid nonlocal density functional theory (DFT), particularly Becke's half and half[30] (BH&H) nonlocal exchange and Lee−Yang−Parr[31] (LYP) nonlocal correlation functionals, has previously been found to be sufficiently accurate for predicting the transition-state properties.[32,33] Note within the RC-TST framework as discussed above only the relative barrier heights are needed. Our previous studies have shown that the relative barrier heights for hydrogen abstraction reactions can be accurately predicted by the BH&HLYP method.[23,25,26,34] Geometries of reactants, transition states, and products were optimized at the BH&HLYP level of theory with the Dunning's correlation-consistent polarized valence double-ζ basis set [3s2p1d/2s1p] denoted as cc-pVDZ, which is sufficient to capture the physical change along the reaction coordinate for this type of reaction. Normal mode analysis was performed at each stationary point to ensure its characteristics, i.e., the stable structure has zero imaginary vibrational frequency, whereas the transition-state (TS) structure has one imaginary vibrational frequency whose mode corresponds to the reaction coordinate of the reaction being considered. Geometry, energy, and frequency information were used to derive the RC-TST factors. The AM1 semiempirical method was also employed to calculate the reaction energies of the reactions considered here. AM1 and BH&HLYP/cc-pVDZ reaction energies were then used to derive the LER's between the barrier heights and reaction energies. Note that AM1 reaction energy is only used to derive the LER's for extracting accurate barrier height and is not directly involved in any rate calculation.

For the reference reaction the minimum energy path (MEP) is obtained at the BH&HLYP/cc-pVDZ level using the Gonzalez−Schlegel method[35] in the mass-weighted Cartesian coordinates with a step size of 0.01 $(amu)^{1/2}$ bohr. Force constants at 300 points along the MEP were determined to ensure convergence of the small curvature tunneling calculations. The points were chosen based on the curvatures of the MEP and the geometrical parameters as a function of the reaction coordinate according to our autofocusing technique.[36] Energetic information along the MEP is further refined by single-point calculations using the coupled cluster method including single and double excitations with a quasi-perturbative triples contribution [CCSD(T)] with the cc-pVDZ basis set at the BH&HLYP/cc-pVDZ geometry, which is denoted as [CCSD(T)/cc-pVDZ//BH&HLYP/cc-pVDZ]. The CCSD(T) energies combined with the BH&HLYP/cc-pVDZ geometries and frequencies were then used for rate constant calculations of the reference reaction.

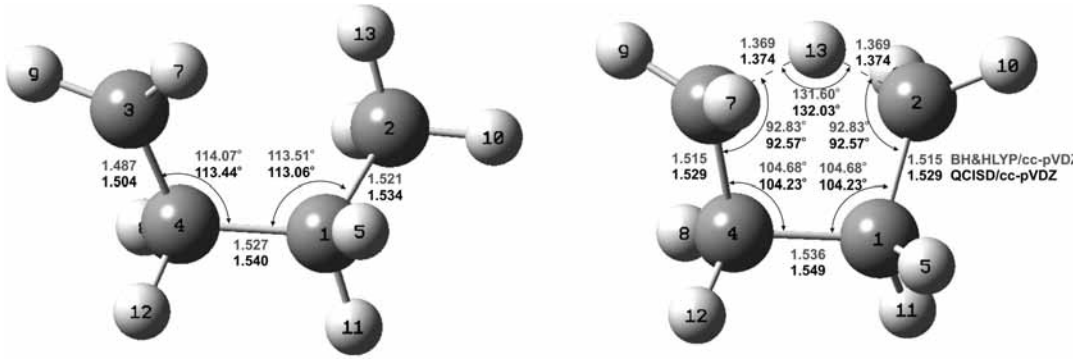

Figure 1. Optimized geometries (distances in Å and angles in degrees) of the reactant C_4H_9 and transition state at the BH&HLYP/cc-pVDZ and QCISD/cc- pVDZ (bold numbers).

To derive the RC-TST correlation functions TST/Eckart rate constants for all reactions in the representative set were calculated. All kinetic calculations were done using the kinetic module of the web-based Computational Science and Engineering Online (CSE-Online) environment.[37] In these calculations overall rotations were treated classically and vibrations treated quantum mechanically within the harmonic approximation except for the modes corresponding to the internal rotations of the CH_2, CH_3, and C_2H_5 groups, which were treated as hindered rotations using the method of Ayala et al.[38] Thermal rate constants were calculated for the temperature range from 300 to 3000 K, which is sufficient for many combustion applications.

Results and Discussion

In the discussion below the rate constants for the reference reaction are presented first and then we describe how the RC-TST factors were derived using the representative reaction set. Subsequently, several error analyses were performed in order to provide some estimates on the accuracy of the RC-TST method applied to this reaction class. The first error analysis is the direct comparison between the calculated rate constants with those available in the literature. The second error analysis is a comparison between rate constants calculated by the RC-TST method and those from explicit full TST/Eckart calculations for the whole set. Final analysis is on the systematic errors from using fitted analytical expressions for the RC-TST correlation functions.

3.1. Kinetics of 1,4-H Shift in *n*-Butyl Radical. The first task for applying the RC-TST method to any reaction class is to have rate constants of the reference reaction as accurate as possible. The rate constants can be from either experimental data or first-principles calculations. In this study the principal reaction is chosen as the smallest reaction in all training sets, namely, a 1,4-shift in the butyl radical (R1). Because of its small size its rate constants can be calculated accurately using canonical variational transition state theory (CVT) with the small curvature tunneling (SCT) method for the temperature range of 300−3000 K.

3.1.1. Stationary Points. The optimized geometrical parameters of the reactant (C_4H_9) and transition state at the BH&HLYP/cc-pVDZ and QCISD/cc-pVDZ levels of theory are shown in Figure 1. Results show that the BH&HLYP/cc-pVDZ method predicts geometries close to those from the QCISD/cc-pVDZ level of theory for the reactant and transition state with the largest difference of 0.014 Å. Similarly, for frequencies the average absolute difference is about 32 cm^{-1} between those from the BH&HLYP/cc-pVDZ and QCISD/ cc-pVDZ calculations. This leads to differences in the total ZPE's of 1.48 and 1.45 kcal/mol for the reactant and transition state, respectively. However, the differences between the two levels on the ZPE corrections to the classical barrier height and reaction energy are insignificant (i.e., less than 0.05 kcal/mol.).

TABLE 2: Calculated Barrier Height and Reaction Energy for the C•CCC → CCCC• Reaction (numbers are in kcal/mol)[a]

level of theory	ΔV (kcal/mol)
BH&HLYP/cc-pVDZ	26.9
CCSD(T)/cc-pVDZ//BH&HLYP/cc-pVDZ	24.8
CBS-QB3[35]	24.2
MP2/6-311G**//HF/6-31G*[19]	26.4

[a] Zero-point energy correction is included.

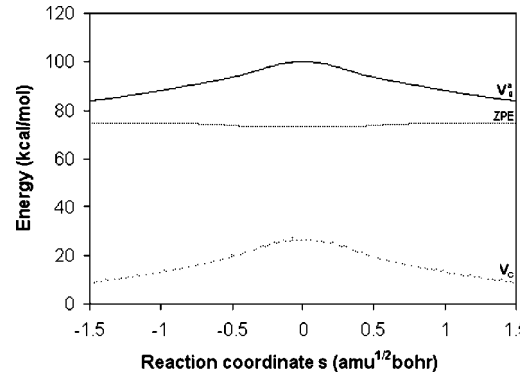

Figure 2. Potential-energy curves along the reaction coordinates of the C•CCC → CCCC• reaction. V_g^a is the vibrationally adiabatic ground-state potential curve, V_C is the classical adiabatic ground-state potential curve, and ZPE is the vibrational zero-point energy.

The classical barrier heights of the reference reaction calculated at various levels of theory with inclusion of ZPE corrections are listed in Table 2. Consistent with our previous work,[23−25] the BH&HLYP/cc-pVDZ method gives rather accurate results, comparable to those obtained with more advanced and expensive correlation methods. In fact, these data are consistent with those reported by Viskolcz et al.[19] with a difference of about 0.5 kcal/mol. From Table 2 the compound method CBS-QB3[39] is expected to yield the most accurate result for the barrier height, namely, 24.2 kcal/mol. This result is very close to that from the CCSD(T)/cc-pVDZ//BH&HLYP/cc-pVDZ level. Consequently, for computing efficiency reasons, the CCSD(T)/cc-pVDZ//BH&HLYP/cc-pVDZ method is used to correct the energy along the minimum energy path for rate calculations discussed below.

Figure 2 illustrates the potential-energy surface for this reaction. The zero-point energy, ZPE, was calculated using

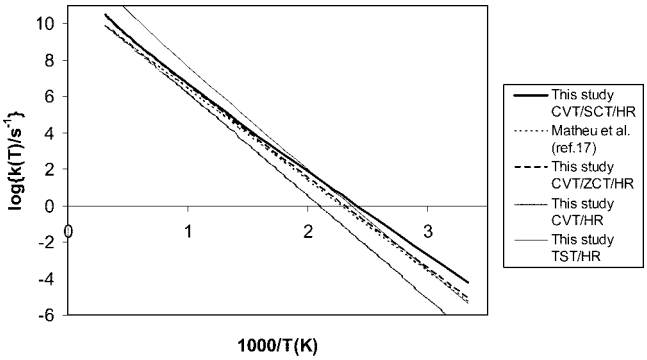

Figure 3. Arrhenius plot of the calculated rate constants for the C•CCC → CCCC• reaction along with those available in the literature.

BH&HLYP/cc-pVDZ frequencies. The classical adiabatic ground-state potential V_c values were obtained from CCSD (T)/cc-pVDZ//BH&HLYP/cc-pVDZ calculations, and the vibrationally adiabatic ground-state potential curve, V^a_g, were the sum product of the two terms V_c + ZPE. The ZPE correction lowers the classical barrier height about 1%. Moreover, the ZPE profile is rather flat in the vicinity of the transition state.

3.1.2. Rate Constants. The rate constants of the reference reaction were calculated using canonical variational transition-state theory (CVT) with small curvature tunneling (SCT) over a wide range of temperatures from 300 to 3000 K. The greatest computational challenge of multidimensional tunneling methods is the rather large number of force constant matrices for points along the MEP. A reaction symmetry number of 3 was used to account for the number of symmetrically equivalent reaction paths. Three low-frequency modes correspond to rotations of the CH_2, CH_3, and C_2H_5 groups in the reactant, and points along the MEP are treated as hindered rotors. The final CVT/SCT/HR rate constants are plotted in Figure 3 and fitted to an Arrhenius expression, given as

$$k_r = (1.33698 \times 10^6) T^{1.62719} \exp\left(-\frac{9933.43}{T}\right) \qquad (7)$$

The TST/HR, CVT/HR, and CVT/ZCT/HR rate constants were also plotted for comparison purposes. Differences in CVT and CVT/ZCT-SCT rate constants indicate a rather significant tunneling contribution at low temperatures. Tunneling effects become less important when $T > 1000$ K.

To the best of our knowledge, there is no experimental kinetic study on this reaction. The only data available in the NIST[40] database is based on the DFT calculations performed by Mathieu et al.[21] The reaction rate was obtained using TST theory with tunneling and hindered rotation corrections. Thus, it is expected that the results presented here would be more accurate. In the high-temperature regime ($T > 1000$ K) these results are almost identical to the CVT rates presented. For lower temperatures, however, the differences are already noticeable but not very significant. These differences are due to the more accurate tunneling treatments used in our calculations.

3.2. Reaction Class Parameters. This section describes how the RC-TST factors were derived using the representative reaction set.

3.2.1. Potential-Energy Factor. The potential-energy factor can be calculated using eq 6, where $\Delta V_a^{\ddagger}$ and $\Delta V_r^{\ddagger}$ are the barrier heights of the arbitrary and reference reactions, respectively. It has been shown previously that within a given class there is a linear energy relationship (LER) between the barrier height and the reaction energy, similar to the well-known Evans−Polanyi linear free-energy relationship.[41−43] Thus, with a LER accurate barrier heights can be predicted from only the reaction energies. In this study, the LER is determined, where the reaction energy can be calculated by either the AM1 or the BH&HLYP level of theory. Alternatively, it is possible to approximate all reactions at the same type of carbon atom site as having the same barrier height, namely, the average value. In previous studies[26,34] this approximation was referred to as the barrier height grouping (BHG) approximation. It was shown[34] that substitution of an alkyl group will stabilize the radical species, thus lowering the barrier height. Thus, one can expect hydrogen migration reactions from the tertiary carbon to have a lower barrier height than those from a secondary carbon. The same relationship is expected to hold between the H shift from a secondary and primary carbon atom. These expectations were confirmed in our DFT calculation when the average scaled barrier heights for H shift from a primary, secondary, and tertiary carbon are 27.75, 24.44, and 23.18 kcal/mol, respectively. The reaction energies and barrier heights for all representative reactions in the representative set are given explicitly in Table 3. The observed linear energy relationships plotted against the reaction energies calculated at the BH&HLYP/cc-pVDZ and AM1 levels are shown in Figure 4a and 4b, respectively. These linear fits were obtained using the least-squares fitting method and have the following expressions

$$\Delta V_a = 0.4915 \Delta E^{\mathrm{BH\&HLYP}} + 26.151(\mathrm{kcal/mol}) \qquad (8a)$$

$$\Delta V_a = 0.2569 \Delta E^{\mathrm{AM1}} + 26.116(\mathrm{kcal/mol}) \qquad (8b)$$

Except for the reference reaction the absolute deviations of reaction barrier heights between the LERs and the direct DFT BH&HLYP/cc-pVDZ calculations are smaller than 0.55 kcal/mol (see Table 3). The mean absolute deviation of reaction barrier heights predicted from BH&HLYP and AM1 reaction energies are 0.21 and 0.45 kcal/mol, respectively. These deviations are, in fact, smaller than the systematic errors of the computed reaction barriers from full electronic structure calculations (see Table 2). This is certainly an acceptable level of accuracy for kinetic modeling. Note that in the RC-TST/LER methodology only the relative barrier height is needed. To compute these relative values the scaled barrier height of the reference reaction R_1 calculated at the same level of theory, i.e., BH&HLYP/cc-pVDZ, is needed and has a value of 26.89 kcal/mol (see Table 3).

On the basis of the observation of barrier heights grouping (BHG) on the three reaction sites the average scaled values are assigned to all reactions in the same type of site, namely, 27.75, 24.44, and 23.18 kcal/mol for primary, secondary, and tertiary carbon sites. The averaged deviations of reaction barrier heights estimated from grouping are 0.37, 0.20, and 0.63 kcal/mol, respectively, which correspond to 1.3%, 0.8%, and 2.7% of the mean barrier height. Therefore, this approach can also be used to estimate the relative barrier height quickly with an acceptable, i.e., less than 3%, deviation. The key advantage of this approach is that it does not require any additional information to estimate rate constants.

In conclusion, the barrier heights for any reaction in this reaction class can be obtained using either the LER or the BHG approach. The estimated barrier height is then used to calculate the potential-energy factor using eq 6. The performance for such estimations on the whole representative reaction set is discussed in the error analyses below.

3.2.2. Reaction Symmetry Number Factor. The reaction symmetry number factors f_σ were calculated simply from the ratio of reaction symmetry numbers of the arbitrary and

TABLE 3: Classical Reaction Energies, Barrier Heights, and Absolute Deviations between Calculated Barrier Heights from DFT and Semi-Empirical Calculations and Those from LER Expressions and BHG Approach[a]

	ΔE		$\Delta V^{\ddagger}$				$\lvert\Delta V^{\ddagger}-\Delta V^{\ddagger}_{\text{estimated}}\rvert$[g]		
reaction	DFT[b]	AM1[c]	DFT[b]	DFT[d]	AM1[e]	BHG[f]	DFT[d]	AM1[e]	BHG[f]
R_1	0.00	0.00	26.88	26.15	26.25	27.75	0.73	0.63	0.87
R_2	3.31	5.14	28.14	27.78	27.58	27.75	0.37	0.57	0.39
R_3	−3.31	−5.14	25.07	24.52	24.92	24.44	0.54	0.14	0.63
R_4	−3.42	−8.22	24.64	24.47	24.13	24.44	0.17	0.51	0.20
R_5	−3.55	−9.47	24.38	24.41	23.81	24.44	0.03	0.57	0.06
R_6	3.55	8.02	27.67	27.89	28.32	27.75	0.22	0.65	0.08
R_7	−5.81	−9.43	23.22	23.29	23.82	23.18	0.07	0.59	0.04
R_8	3.40	9.43	28.07	27.82	28.68	27.75	0.25	0.61	0.32
R_9	−3.32	−4.67	24.36	24.52	25.04	24.44	0.16	0.68	0.08
R_{10}	3.32	4.67	27.44	27.78	27.46	27.75	0.34	0.01	0.31
R_{11}	−4.50	−4.30	23.44	23.94	25.14	23.18	0.50	1.70	0.26
R_{12}	−6.00	−13.19	23.03	23.20	22.85	23.18	0.17	0.18	0.15
R_{13}	4.72	6.98	28.03	28.47	28.05	27.75	0.44	0.02	0.28
R_{14}	−4.72	−7.13	23.64	23.83	24.41	24.44	0.19	0.77	0.79
R_{15}	−3.67	−5.54	24.47	24.35	24.82	24.44	0.12	0.35	0.04
R_{16}	3.67	5.54	27.88	27.95	27.68	27.75	0.07	0.20	0.13
R_{17}	−3.64	−5.54	24.50	24.36	24.82	24.44	0.14	0.32	0.07
R_{18}	3.64	5.54	27.89	27.94	27.68	27.75	0.05	0.21	0.14
R_{19}	−6.18	−13.15	23.04	23.11	22.86	23.18	0.07	0.18	0.14
MAD[h]							0.21	0.45	0.26

[a] Zero-point energy correction is not included. Energies are in kcal/mol. [b] Calculated at the BH&HLYP/cc-pVDZ level of theory and scaled by a factor of 0.93. [c] Calculated at the AM1 level of theory. [d] Calculated from the LER using reaction energies calculated at the BH&HLYP/cc-pVDZ level of theory: eq 9a. [e] Calculated from the LER using reaction energies calculated at the AM1 level of theory: eq 9b. [f] Estimated from barrier height grouping. [g] $\Delta V^{\ddagger}$ from BH&HLYP/cc-pVDZ calculations. $\Delta V^{\ddagger}_{\text{estimated}}$ from the linear energy relationship using BH&HLYP/cc-pVDZ and AM1 reaction energies or from barrier height grouping. [h] Mean absolute deviations (MAD) for reactions R_2-R_{19}.

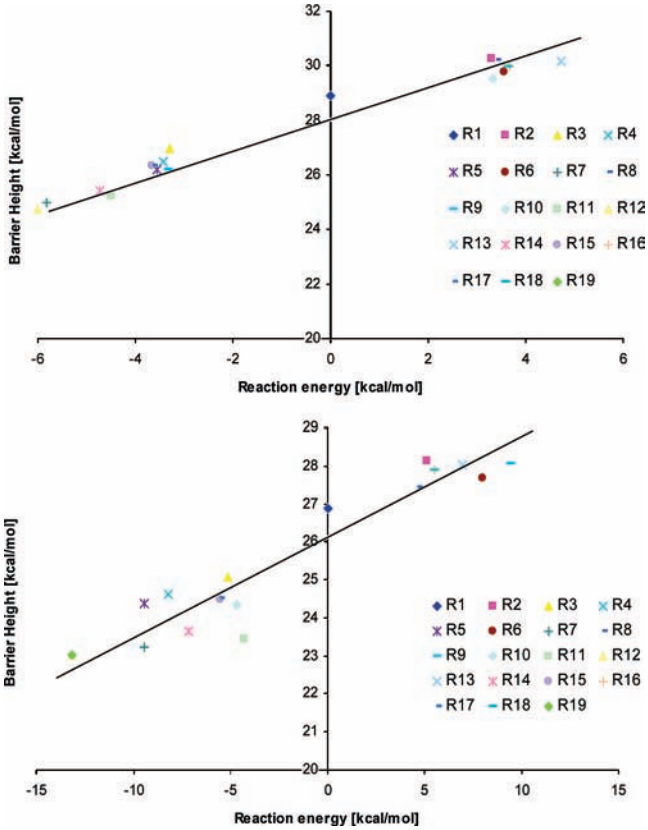

Figure 4. Linear energy relationship plot of the barrier heights, $\Delta V^{\ddagger}$, versus the reaction energies ΔE. Barrier heights were calculated at the BH&HLYP/cc-pVDZ level of theory. ΔE's were calculated at the (a) BH&HLYP/cc-pVDZ and (b) AM1 levels of theory.

TABLE 4: Calculated Symmetry Number Factors and Tunneling Factors at 300 K

		tunneling ratio factor, f_κ			
reaction	symmetry number factor	Eckart[a]	fitting[b]	deviation[c]	%deviation[d]
R_1	1.00	(4088)[f]			
R_2	1.00	0.89	0.71	0.19	20.75
R_3	0.67	0.89	0.75	0.14	16.09
R_4	0.67	0.78	0.75	0.03	4.25
R_5	0.67	0.66	0.75	0.08	12.63
R_6	1.00	0.66	0.71	0.04	6.37
R_7	0.33	0.49	0.50	0.01	1.33
R_7	1.00	0.49	0.71	0.22	44.07
R_9	0.67	0.63	0.75	0.12	19.40
R_{10}	1.00	0.63	0.71	0.08	12.76
R_{11}	0.33	0.55	0.50	0.05	9.17
R_{12}	0.33	0.47	0.50	0.02	5.00
R_{13}	1.00	0.76	0.71	0.05	7.16
R_{14}	0.67	0.76	0.75	0.01	1.70
R_{15}	0.67	0.76	0.75	0.01	1.38
R_{16}	1.00	0.76	0.71	0.05	6.86
R_{17}	0.67	0.75	0.75	0.01	0.71
R_{18}	1.00	0.75	0.71	0.05	6.23
R_{19}	0.33	0.48	0.50	0.02	4.19
MAD[e]				0.07	10.00

[a] Calculated directly using the Eckart method with BH&HLYP/cc-pVDZ reaction barrier heights and energies. [b] Calculated using the fitting expression. [c] Absolute deviation between the fitting and directly calculated values. [d] Percentage deviation (%). [e] Mean absolute deviations (MAD) and deviation percentage between the fitting and the directly calculated values. [f] Tunneling coefficient calculated for reaction R_1 using the Eckart method with the energetic and frequency information at BH&HLYP/cc-pVDZ.

reference reactions using eq 3 and are listed in Table 4. The reaction symmetry number of a reaction is given by the number of symmetrically equivalent reaction paths. For the H-atom intramolecular migration reaction class this number is equal to the number of H atoms connected to the hydrogen abstraction site: 3 for primary carbons, 2 for secondary carbons, and 1 for tertiary carbons. This value is multiplied by the number of equivalent migration sites in the molecule. Reaction 5 can serve

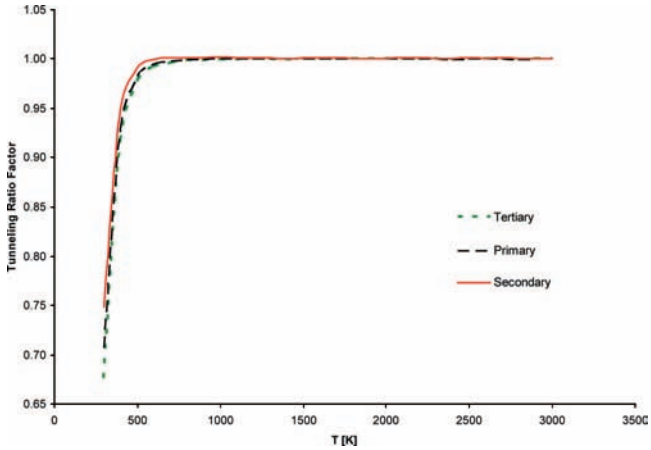

Figure 5. Plots of the tunneling ratio factors f_κ as a function of the temperature for the 1,4-hydrogen migration from primary, secondary, and tertiary carbon sites.

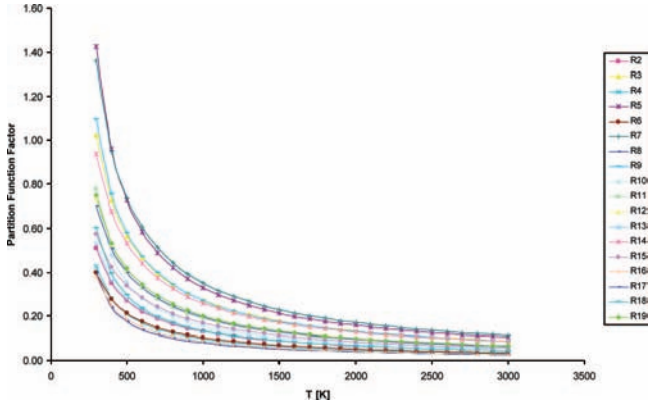

Figure 6. Plots of the total partition function factors for 18 reactions, R_2-R_{19}.

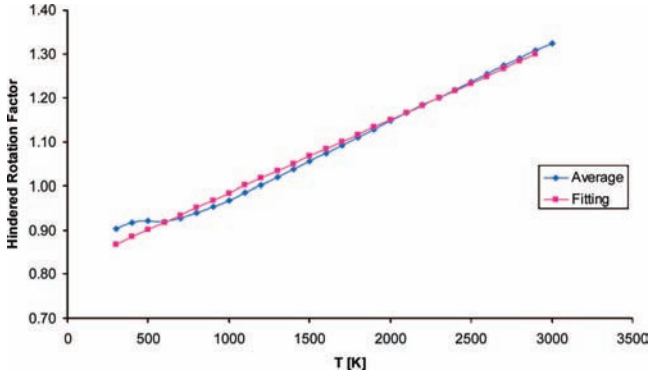

Figure 7. Average hindered rotation corrections to the total rate constants for all reactions in the temperature range of 300−3000 K.

as a useful example here. Because there are two equivalent primary C atoms in the CC(C)CC˙C molecule, the reaction symmetry number is equal to 2 × 3 = 6. In any case, this number can be easily calculated from the molecular topology of the reactant; thus, the symmetry number factor can be calculated exactly.

3.2.3. Tunneling Factor. The tunneling factor f_κ is the ratio of the transmission coefficient of reaction R_a to that of the reference reaction R_r. Due to cancellation of errors in calculations of the tunneling factors we have shown that the factor f_κ can be reasonably estimated using the one-dimensional Eckart method.[24] Calculated results for the representative reaction set can then be fitted to an analytical expression. It is known that

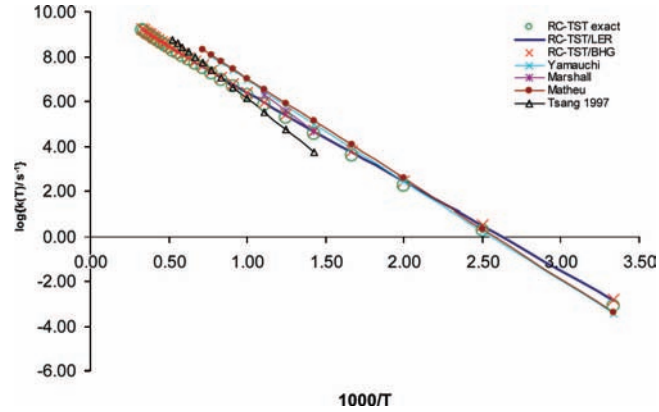

Figure 8. Arrhenius plots of the calculated and literature rate constants using the RC-TST methods for the $CH_3CH_2CH_2CH_2CH_2^\bullet \rightarrow CH_3CH^\bullet CH_2CH_2CH_3$ reaction. Results from using the reaction energies at the BH&HLYP/cc-pVDZ level in the LER are presented.

the tunneling coefficient depends on the barrier height. We have shown that the barrier heights group together into three groups, namely, primary, secondary, and tertiary carbon sites (see Potential-Energy Factor section), it is expected that reactions in the same group have similar tunneling factors and thus the average value can be used for the whole group. Simple expressions for the three tunneling factors for primary, secondary, and tertiary carbon sites are obtained by fitting to the average calculated values and are given below

$$f_\kappa^{\mathrm{I}} = 1 - 19.916\exp(-T/71.103) \text{ for primary carbon sites} \quad (9a)$$

$$f_\kappa^{\mathrm{II}} = 1.002 - 29.278\exp(-T/63.109) \text{ for secondary carbon sites} \quad (9b)$$

$$f_\kappa^{\mathrm{III}} = 0.998 - 15.770\exp(-T/86.944) \text{ for tertiary carbon sites} \quad (9c)$$

The correlation coefficients r^2 for these fits are larger than 0.999. The three equations are plotted in Figure 5, and the error analysis at 300 K is listed in Table 4. It can be seen that the same tunneling factor expression can be reasonably assigned to all reactions at the same site with the largest percentage deviation of 44% for R_7 and the mean absolute deviation of 7% compared to the direct Eckart calculations. At higher temperatures tunneling contributions to the rate constants decrease, and thus, as expected, the differences between the approximated values and the explicitly calculated ones also decrease; for example, the maximum error for all reactions is less than 1% at 500 K.

3.2.4. Partition Function Factor. The partition factor is the product of the translational, rotational, internal rotation, vibrational, and electronic components. The translational and rotational factors are temperature independent. As pointed out in our previous study,[24] the temperature-dependent part of the total partition function factor f_Q mainly originates from the differences in the coupling between the substituents with the reactive moiety and its temperature dependence, which arises from the vibrational component and internal rotations only. Partition function factors for 18 reactions (R_2-R_{19}) in the class calculated in the temperature range 300−3000 K are given in Figure 6. Note that since contributions from the hindered rotation modes are treated separately they are not included in these partition function calculations. Since the variations in factors corresponding to different types of carbon atom sites were found to be

TABLE 5: Parameters and Formulations of the RC-TST Method for the 1,4-Intramolecular Hydrogen Migration in the Alkyl Radicals Reaction Class ($CH_3CH_2CH_2CH_2^{\bullet} \rightarrow CH_2^{\bullet}CH_2CH_2CH_3$ is the reference reaction)[a]

$$k_a(T) = k_p(T)\cdot f_k(T)\cdot f_{HR}(T)\cdot f_v(T)\cdot f_\sigma\,; \quad f_v(T) = \exp\left[\frac{-\Delta V^{\ddagger} - \Delta V_r^{\ddagger}}{k_B T}\right]$$

f_σ	calculated explicitly from the symmetry of reactions (see Table 4)
$f_k(T)$	$f_k^{I} = 1 - 19.916\exp(-T/71.103)$ for primary carbon sites
	$f_k^{II} = 1.002 - 29.278\exp(-T/63.109)$ for secondary carbon sites
	$f_k^{III} = 0.998 - 15.770\exp(-T/86.944)$ for tertiary carbon sites
$f_Q(T)$	$f_Q^{I} = 206.56T\cdot T^{-1.0770}$ for primary carbon sites
	$f_Q^{II} = 346.82T\cdot T^{-1.0590}$ for secondary carbon sites
	$f_Q^{III} = 343.53T\cdot T^{-1.0522}$ for tertiary carbon sites
$f_{HR}(T)$	$f_{HR} = (3.69 \times 10^{-4})T + 0.818$
$\Delta V^{\ddagger}$	LER
	$\Delta V_a = 0.2569\Delta E^{AM1} + 26.116$
	$\Delta V_r^{\ddagger} = 26.90$ kcal/mol
$k_p(T)$	$k_r = (1.33698 \times 10^{6})T^{1.62719}\exp(-9933.43/T)$ [s^{-1}]
BHG approach	$k(T) = (2.692 \times 10^{8})T^{0.558}\exp(-9403.916/T)$ for primary carbon sites
	$k(T) = (4.789 \times 10^{8})T^{0.517}\exp(-7778.518/T)$ for secondary carbon sites
	$k(T) = (1.098 \times 10^{9})T^{0.340}\exp(-7392.211/T)$ for tertiary carbon sites

[a] T is in Kevin; $\Delta V^{\ddagger}$and ΔE are in kcal/mol; zero-point energy correction is not included.

rather significant we derived different formulas for migration from primary, secondary, and tertiary carbon atom separately. The average values for the H shift from primary, secondary, and tertiary carbon sites were fitted into analytical expressions as given below

$$f_Q^{I} = 206.56T\cdot T^{-1.0770} \text{ for primary carbon sites} \quad (10a)$$

$$f_Q^{II} = 346.82T\cdot T^{-1.0590} \text{ for secondary carbon sites} \quad (10b)$$

$$f_Q^{III} = 343.53T\cdot T^{-1.0522} \text{ for tertiary carbon sites} \quad (10c)$$

The correlation coefficients r^2 for these fits are larger than 0.99. As one may see from Figure 6 the average value of the partition function factor for $T > 1000$ K differs substantially from unity for all reactions in the representative set. As mentioned earlier, the coupling between substituents with the reactive moiety is believed to account for these differences.

3.2.5. Hindered Rotation Factor. For this reaction class rotations of the alkyl (for example, CH_3) or alkanyl (CH_2) groups along the C−C bond for some reactants, transition states, and products need to be treated as hindered rotors. We used the approach proposed by Ayala et al.[38] The reaction class factor due to these hindered rotors is a measure of the substituent effects on the rate constants from these hindered rotors relative to that of the reference reaction. The effect of the hindered rotation treatment to total rate constants can be seen in Figure 7. For the sake of simplicity and clarity only the average factor for each reaction is presented. It can be seen from Figure 7 that the HR correction factors are dependent on the temperature. The average values at temperatures below 1000 K are smaller than 1, whereas, for $T > 2000$ K the average factor is significantly higher than 1. The average values, as applied to the whole class, are fitted into a linear expression with $r^2 > 0.99$, as given below

$$f_{HR} = (3.69\times10^{-4})T + 0.818 \quad (11)$$

3.3. Prediction of Rate Constants. What we have established so far are the necessary parameters, namely, potential-energy factor, reaction symmetry number factor, tunneling factor, and partition function factor, for application of the RC-TST theory to predict rate constants for any reaction in the 1,4-intramolecular hydrogen migration class. The procedure for calculating rate constants of an arbitrary reaction in this class is (i) calculate the potential-energy factor using eq 6 with a $\Delta V_r^{\ddagger}$ value of 28.91 kcal/mol. The reaction barrier height can be obtained using the LER approach by employing eq 8a for BH&HLYP/cc-pVDZ or eq 8b for AM1 reaction energies or by the BHG approach, (ii) calculate the symmetry number factor from eq 3 or see Table 4, (iii) compute the tunneling factor using eq 9a, 9b, or 9c for primary, secondary, and tertiary carbon sites, respectively, (iv) evaluate the partition function factor using eqs 10a, 10b, and 10c, (v) evaluate the hindered rotation factor using eq 11, and (vi) the rate constants of the arbitrary reaction can be calculated by taking the product of the reference reaction rate constant given by eq 7 with the reaction class factors above. Table 5 summarizes the RC-TST parameters for this reaction class.

If the BHG barrier heights and average values for other factors are used the rate constants are denoted by RC-TST/BHG. The RC-TST/BHG rate constants for any reactions belonging to this class can be estimated without any further calculations as

$$k(T) = (2.692\times10^{8})T^{0.558}\exp\left(\frac{-9403.916}{T}\right)(s^{-1})$$

for primary carbon sites (12a)

$$k(T) = (4.789\times10^{8})T^{0.517}\exp\left(\frac{-7778.518}{T}\right)(s^{-1})$$

for secondary carbon sites (12b)

$$k(T) = (1.098\times10^{9})T^{0.340}\exp\left(\frac{-7392.211}{T}\right)(s^{-1})$$

for tertiary carbon sites (12c)

The appropriate symmetry factor of 3 for primary carbon sites, 2 for secondary carbon sites, and 1 for tertiary carbon sites are included in the rate constant expressions above. Correction for the number of equivalent migration sites depends on the specific reaction and thus must be included explicitly.

3.4. Error Analyses. As mentioned earlier, only a limited amount of the experimental data is available for intramolecular H shift in alkyl radicals. *n*-Pentyl (reaction R_3) and *n*-octyl isomerizations (reactions R_{13}−R_{14}) are used to illustrate the

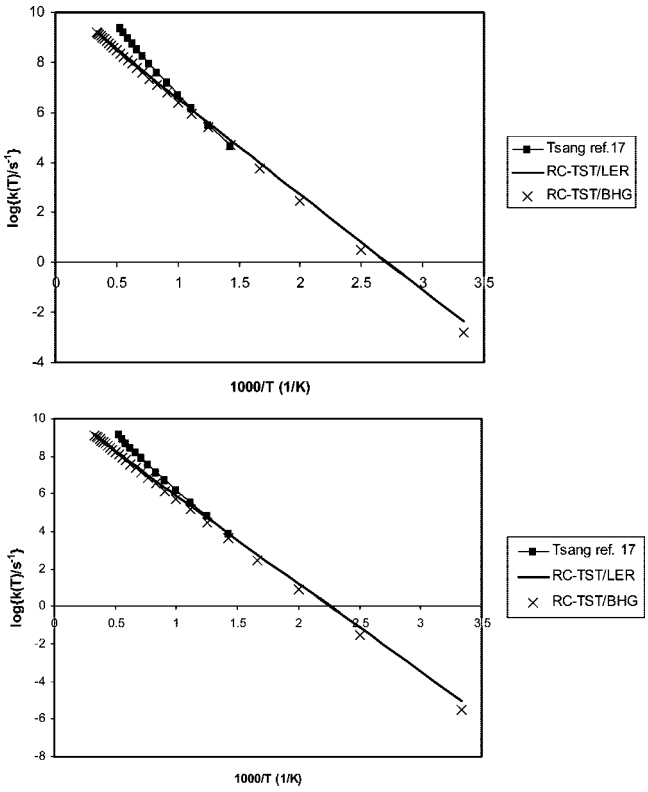

Figure 9. Arrhenius plots of the calculated and experimental rate constants for the (a) 1-octyl→ 4-octyl (R_{13}) and (b) 4-octyl → 1-octyl (R_{14}) reactions. Calculated RC-TST results using the reaction energies at the BH&HLYP/cc-pVDZ level in the LER are presented.

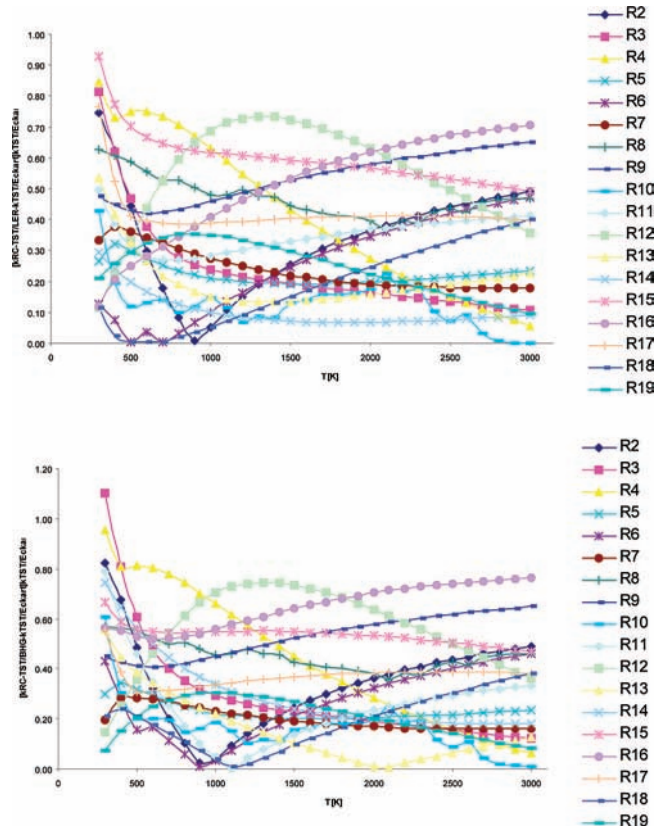

Figure 10. Relative absolute deviations as a function of the temperature between rate constants calculated from explicit TST/Eckart calculations for all selected reactions and (a) from the RC-TST/LER method where BH&HLYP reaction energies were used for the LER and (b) from the RCT-TST/BHG method.

theory. It is noted that there is no direct experimental data available for the R_3 reaction, but some were derived from experiments.[13,44] Figure 8 shows the predicted rate constant of reaction R_3 using the RC-TST method and literature data.[13,15,21,44] In this figure the "RC-TST exact" notation means that the reaction class factors were calculated explicitly rather than using the approximate expressions listed in Table 5. Because there are not big differences between the results obtained from using either the BH&HLYP/cc-pVDZ or AM1 reaction energies only rate constants from BH&HLYP are presented here. As can be seen from Figure 8 the agreement between the predicted results and experimentally derived data is, for reaction R3, quite excellent.

Figure 9a,b shows the comparison of the our RC-TST/LER and RC-TST/BHG reaction rates with the newest measurements available by Tsang and co-workers.[14] These experiments were performed in a single-pulse shock tube at temperatures in the 850−1000 K range. High-pressure rate constants have been derived over 700−1900 K range with an uncertainty factor of 2. Figure 9a shows rates for reaction R_{14} from the training set (1-octyl = 4-octyl), whereas Figure 9b shows rates for reaction R_{13} (4-octyl = 1-octyl), which is the inverse reaction to R_{14}. These figures show that the agreement between theory and experiment is excellent. In fact, the RC-TST rates are within the uncertainty factor with the measurement values for the temperature range of the experiments performed (850−1000 K) and lower (700−850 K). The same is also true for extrapolation of Tsang's data from 700 to 300 K (this extrapolation is not shown in Figure 9). For temperatures higher than 1200 K the differences are more noticeable.

The second error analysis provides a systematic analysis on the efficiency of the RC-TST method by comparing RC-TST results with those from explicit calculations. As mentioned in our previous studies,[22,24,45] the RC-TST methodology can be thought of as a procedure for extrapolating rate constants of the reference reaction to those of any reaction in the class. Comparisons between the calculated rate constants for a small number of reactions using both the RC-TST and the full TST/Eckart methods provide additional information on the accuracy of the RC-TST method. To be consistent, the TST/Eckart rate constants of the reference reaction were used in calculation of RC-TST rate constants for this particular analysis rather than using the expression in eq 7. The results for this error analysis for 18 representative reactions (i.e., the comparisons between the RC-TST/LER and full TST/Eckart methods) are shown in Figure 10a, wherein the relative deviation defined by ($k^{\mathrm{TST/Eckart}} - k^{\mathrm{RC\text{-}TST/LER}}/k^{\mathrm{TST/Eckart}}$) as a percent versus the temperature for all reactions in the representative set, R_2-R_{19} is plotted. For the temperatures >1000 K for most of the reactions in this set, 15 out of 18, the unsigned relative errors are within 60%. In the low-temperatures regime five reactions have errors larger than 60%. Thus, in general, it can be concluded that RC-TST can estimate thermal rate constants for reactions in this class within 60% when compared to those calculated explicitly using the TST/Eckart method. For other cases maximum error is less than 95%, which is still an acceptable level of accuracy for reaction engineering purposes. It is noted that this analysis is presented for RC-TST/LER only. One would expect slightly worse performance for the RC-TST/BHG approach as shown in Figure 10b, wherein the maximum error exceeds 100%. As expected, these differences are only minor and do not significantly affect the accuracy of the RC-TST method. The convenience of ready to be used rate expressions for any reaction

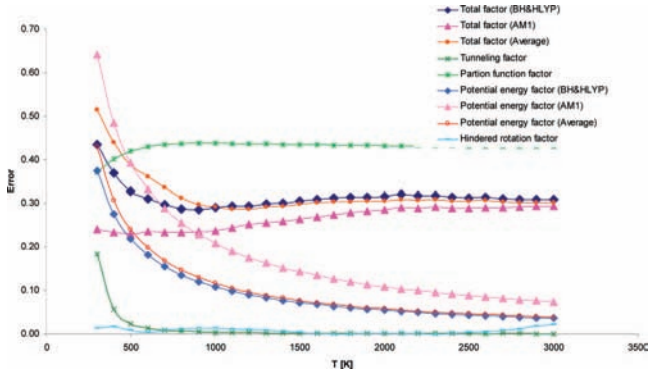

Figure 11. Averaged absolute errors of the total relative rate factors $f(T)$ (eq 2) and its components, namely, the tunneling (f_K), partition function (f_Q), and potentialienergy (f_V) factors as a function of temperature.

in the class would offset the lower accuracy of the BHG approach compared to that of the LER.

Finally, an analysis of the systematic errors in different factors in the RC-TST/LER methods was performed. The total error is affected by the errors in the approximations in the potential-energy factor, tunneling factor, and partition function factor introduced in the method. The deviations/errors between the approximated and exact factors within the TST framework are calculated at each temperature for every reaction in the representative set and then averaged over the whole class. For the LER approach, error in the potential-energy factor comes from - use of an LER expression, that of the tunneling factor from three equations (eqs 9a, 9b, and 9c), that of the partition function factor from using eqs 10a, 10b, and 10c, and that of the hindered rotation factor from using eq 11. Absolute errors averaged over all 18 reactions, R_2-R_{19} as a function of the temperature are plotted in Figure 11. Of the factors the hindered rotation (HR) and partition function ratios factor show the least temperature dependence for the whole temperature range. The HR factor introduced the smallest error of less than 4%, while the error introduced by the partition function factor is the largest of the individual factors for $T > 300$ K, roughly around 50% for the whole temperature range. As mentioned earlier, this significant error is caused by a very small (less than 0.1) value of the partition factor for $T > 1000$ K. Only for $T = 300$ K is the error of the BHG potential-energy factor noticeable. This affects the low-temperature ($T < 700$ K) behavior of the total BHG factor, which exceeds 100% for $T = 300$ K. Thus, the LER approach gives less error in the potential-energy factor than the BHG, though for $T > 700$ K total systematic errors of both LER and BHG factors are almost the same. For temperatures $T > 1000$ K all errors are almost constant. Except for the BHG approach, the total systematic errors due to the use of simple analytical expressions for different reaction class factors are less than 60% for the temperature range 300−3000 K.

In general, if accurate rate constants are needed the RC-TST/LER is recommended, while the BHG methods gives a quick estimation without doing any calculations but with larger errors.

Conclusions

Application of reaction class transition-state theory combined with the linear energy relationship and the barrier height grouping approach to prediction of thermal rate constants for the hydrogen 1,4-intramolecular hydrogen migration reaction class was carried out. The rate constants for the reference reaction $CH_3CH_2CH_2CH_2^{\bullet} \rightarrow CH_2^{\bullet}CH_2CH_2CH_3$ were obtained by the CVT/SCT method in the temperature range 300−3000 K. The RC-TST/LER, where only reaction energy is needed, and RC-TST/BHG, where no other information is needed, are found to be promising methods for predicting rate constants for any reaction in this reaction class. The error analyses indicate that both the RC-TST/LER and the RC-TST/BHG methods can predict rate constants within a factor of 2 compared to explicit rate calculations.

References and Notes

(1) Benson, S. W. *Thermochemical Kinetics*, 2nd ed.; Wiley: New York, 1976.
(2) Miller, J. A.; Knee, R.; Westbtook, C. K. *Annu. Rev. Phys. Chem.* **1990**, *41*, 317.
(3) Curran, H. J.; Gaffuri, P.; Pitz, W. J.; K., W. C. *Combust. Flame* **1998**, *114*, 149.
(4) Curran, H. J.; Gaffuri, P.; Pitz, W. J.; Westbrook, C. K. *Combust. Flame* **2002**, *129*, 253.
(5) Dobe, S.; Berces, T.; Marta, F. *Int. J. Chem. Kinet.* **1987**, 19.
(6) Walker, R. W. *Specialis Periodical reports, Reaction Kinetics*; The Chemical Society; 1975; Vol. 1.
(7) Watkins, K. W. *J. Phys. Chem.* **1973**, *77*, 2938.
(8) Watkins, K. *Can. J. Chem.* **1972**, *50*, 3738.
(9) Le Roy, R. *J. Phys. Chem.* **1980**, *84*, 3508.
(10) Hardwidge, E. A.; Larson, C. W.; Rabinovitch, B. S. *J. Am. Chem. Soc.* **1970**, *92*, 3278.
(11) Larson, C. W.; Chua, P. T.; Rabinovitch, B. S. *J. Phys. Chem.* **1972**, *76*, 2507.
(12) Dobe, S.; T., B.; Reti, F.; Marta, P. *Int. J. Chem. Kinet.* **1987**, *19*, 895.
(13) Marshall, R. M. *Int. J. Chem. Kinet.* **1990**, *22*, 935.
(14) Tsang, W.; McGivern, W. S.; Manion, J. A. *Proc. Combust. Inst.* **2009**; doi:10.1016/j.proci.2008.05.048.
(15) Tsang, W.; Bedanov, V.; Zachariah, M. R. *Beri. Bunsen-Ges.* **1997**, *101*, 491.
(16) Tsang, W.; Walker, J. A.; Manion, J. A. *Proc. Combust. Inst.* **2007**, *31*, 141.
(17) Tsang, W.; A.A., I.; Manion, J. A. Multi-channel Decomposition of Heptyl Radicals. *Proceedings of the Third Joint Meeting of the U.S. Sections of the Combustion Institute*, Chicago, IL, 2003.
(18) McGivern, W. S.; Awan, I. A.; Tsang, W.; Manion, J. A., **2008**.
(19) Viskolcz, B.; Lendvay, G.; Körtvélyesi, T.; Seres, L. *J. Am. Chem. Soc.* **1996**, *118*, 3006.
(20) Viskolcz, B.; Lendvay, G.; Seres, L. *J. Phys. Chem. A* **1997**, *101*, 7119.
(21) Matheu, D. M.; Green, W. H.; Grenda, J. M. *Int. J. Chem. Kinet.* **2003**, *35*, 95.
(22) Truong, T. N. *J. Chem. Phys.* **2000**, *113*, 4957.
(23) Kungwan, N.; Truong, T. N. *J. Phys. Chem. A* **2006**, *109*, 7742.
(24) Zhang, S.; Truong, T. N. *J. Phys. Chem. A* **2003**, *107*, 1138.
(25) Huynh, L. K.; Ratkiewicz, A.; Truong, T. N. *J. Phys. Chem. A* **2006**, *110*, 473.
(26) Huynh, L. K.; Zhang, S.; Truong, T. N. *Combust. Flame* **2008**, *152*, 177.
(27) Huynh, L. K.; Barriger, K.; Violi, A. *J. Phys. Chem A* **2008**, *112*, 1436.
(28) Truong, T. N.; Duncan, W. T.; Tirtowidjojo, M. *Phys. Chem. Chem. Phys.* **1999**, *1*, 1061.
(29) Frisch, M. J.; Trucks, G. W.; Schlegel, H. B.; Scuseria, G. E.; Robb, M. A.; Cheeseman, J. R.; Montgomery, J. A.;, Jr.; Kudin, K. N.; Burant, J. C.; Millam, J. M.; Iyengar, S. S.; Tomasi, J.; Barone, V.; Mennucci, B.; Cossi, M.; Scalmani, G.; Rega, N.; Petersson, G. A.; Nakatsuji, H.; Hada, M.; Ehara, M.; Toyota, K.; Fukuda, R.; Hasegawa, J.; Ishida, M.; Nakajima, T.; Honda, Y.; Kitao, O.; Nakai, H.; Klene, M.; Li, X.; Knox, J. E.; Hratchian, H. P.; Cross, J. B.; Adamo, C.; Jaramillo, J.; Gomperts, R.; Stratmann, R. E.; Yazyev, O.; Austin, A. J.; Cammi, R.; Pomelli, C.; Ochterski, J. W.; Ayala, P. Y.; Morokuma, K.; Voth, G. A.; Salvador, P.; Dannenberg, J. J.; Zakrzewski, V. G.; Dapprich, S.; Daniels, A. D.; Strain, M. C.; Farkas, O.; Malick, D. K.; Rabuck, A. D.; Raghavachari, K.; Foresman, J. B.; Ortiz, J. V.; Cui, Q.; Baboul, A. G.; Clifford, S.; Cioslowski, J.; Stefanov, B. B.; Liu, G.; Liashenko, A.; Piskorz, P.; Komaromi, I.; Martin, R. L.; Fox, D. J.; Keith, T.; Al-Laham, M. A.; Peng, C. Y.; Nanayakkara, A.; Challacombe, M.; Gill, P. M. W.; Johnson, B.; Chen, W.; Wong, M. W.; Gonzalez, C.; Pople, J. A. *Gaussian 03*, Revision A.1; Gaussian, Inc.: Pittsburgh, PA, 2003.
(30) Becke, A. D. *J. Chem. Phys.* **1993**, *98*, 1372.
(31) Lee, C.; Yang, W.; Parr, R. G. *Phys. Rev.* **1988**, *37*, 785.

(32) Truong, T. N.; Duncan, W. *J. Chem. Phys.* **1994**, *101*, 7408.
(33) Lynch, B. J.; Fast, P. L.; Harris, M.; Truhlar, D. G. *J. Phys. Chem. A* **2000**, *104*, 4811.
(34) Huynh, L. K.; Panasewicz, S.; Ratkiewicz, A.; TN, T. *J. Phys. Chem. A* **2007**, *111*, 2035.
(35) Gonzalez, C.; Schlegel, H. B. *J. Phys. Chem.* **1990**, *94*, 5523.
(36) Duncan, W. T.; Bell, R. L.; Truong, T. N. *J. Comput. Chem.* **1998**, *19*, 1039.
(37) Truong, T. N., CSEO.
(38) Ayala, P. Y.; Schlegel, H. B. *J. Chem. Phys.* **1998**, *108*, 2314.
(39) Ochterski, J. W.; Petersson, G. A.; Montgomery, J. A., Jr. *J. Chem. Phys.* **1996**, *104*, 2598.
(40) NIST. Kinetic Database; http://kinetics.nist.gov/.
(41) Evans, M. G.; Polanyi, M. *Proc. R. Soc.* **1936**, *154*, 133.
(42) Evans, M. G.; Polanyi, M. *Trans. Faraday Soc.* **1936**, *32*, 1333.
(43) Polanyi, J. C. *Acc. Chem. Res.* **1972**, *5*, 161.
(44) Yamauchi, N.; Miyoshi, A.; Kosaka, K.; Koshi, M.; Matsui, H. *J. Phys. Chem. A* **1999**, *103*, 2723.
(45) Truong, T. N.; Maity, D. K.; Truong, T.-T. T. *J. Chem. Phys.* **2000**, *112*, 24.

JP808874J